Chemosphere 293 (2022) 133601

Contents lists available at ScienceDirect

Chemosphere

journal homepage: www.elsevier.com/locate/chemosphere

Iron carriers promote biofilm formation and *p*-nitrophenol degradation

Lifeng Cao [a,b], Ge Zhu [a], Jinzhao Tao [a], Yongming Zhang [a,*]

[a] Department of Environmental Science and Engineering, School of Environmental and Geographical Science, Shanghai Normal University, Shanghai, 200234, PR China
[b] School of Environment and State Key Joint Laboratory of Environment Simulation and Pollution Control, Tsinghua University, Beijing, 100084, China

HIGHLIGHTS

- Fe-carriers can promote biofilm formation and PNP degradation.
- More iron uptake genes were expressed under iron-limited conditions.
- Plastic-VBBR had a lower community diversity than Fe-VBBR.
- *Achromobacter* genus and Xanthobacteraceae family may be as PNP degraders.

GRAPHICAL ABSTRACT

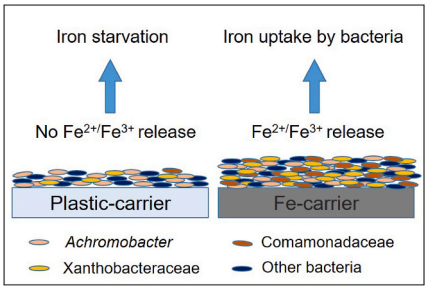

ARTICLE INFO

Handling Editor: Chang-Ping Yu

Keywords:
Biofilm
p-nitrophenol (PNP)
Biofilm carrier
Iron and plastic
Community biodiversity

ABSTRACT

Vertical baffled biofilm reactors (VBBR) equipped with Plastic-carriers and Fe-carriers were employed to explore the effect of biofilm carriers on biofilm formation and *p*-nitrophenol (PNP) degradation. The results showed that Fe-carriers enhanced biofilm formation and PNP degradation. The maximum thickness of biofilm grown on the Fe-carriers was 1.5-fold higher than that on the Plastic-carriers. The Fe-VBBR reached a maximum rate of PNP removal at 13.02 μM L^{-1} h^{-1} with less sodium acetate addition (3 mM), while the maximum rate of PNP removal was 11.53 μM L^{-1} h^{-1} with more sodium acetate addition (6 mM) in the Plastic-based VBBR. High-throughput sequencing suggested that the Fe-VBBR had a higher biodiversity of the bacterial community in evenness, and the *Achromobacter* genus and Xanthobacteraceae family were as main PNP degraders. Kyoto Encyclopedia of Genes and Genomes (KEGG) Orthology analysis suggested more abundances of iron uptake genes were expressed to transport iron into the cytoplasm under an iron-limited condition in two VBBRs, and the metabolic pathway of PNP degradation went through 4-nitrocatechol and 1,2,4-benzenetriol. Our results provide a new insight for iron enhancing biofilm formation and PNP degradation.

1. Introduction

Biofilms are consisted of groups of bacteria attached to surfaces and encased in hydrated extracellular polymeric substances (EPS) (Flemming and Wingender, 2010). Biofilm-based techniques have been recognized for their scalability, robustness, and usefulness in removing a wide array of contaminants from groundwater and surface water (Dutta et al., 2005; Liang et al., 2021). Biofilms can offer advantages, with respect to suspended single cells, in downstream processing by facilitating cell-liquid separation, protection from harmful conditions, utilization of cooperative benefits (community), and long solids retention time (Mitchell et al., 2015; Tan et al., 2021; Wang et al., 2002).

* Corresponding author.
E-mail address: zhym@shnu.edu.cn (Y. Zhang).

https://doi.org/10.1016/j.chemosphere.2022.133601
Received 9 June 2021; Received in revised form 14 December 2021; Accepted 10 January 2022
Available online 13 January 2022

The mechanism of biofilm development has been fully studied for preventing membrane fouling and bacterial infections (Jamal Khan et al., 2012; Kim, 2016; Liu et al., 2017). Although the motivations for investigating biofilm development mainly focused on anti-biofilm in medicine, the establishment of robust biofilm is very crucial to contaminants removal in environmental engineering (Long et al., 2018; Rittmann, 2018; Torresi et al., 2016). In the field of remediation, studies have extensively investigated the efficiency and ability of pollutants removal in various biofilm systems (de Beer et al., 1994; Kwok et al., 1998; Tsushima et al., 2007). Additionally, biofilm carriers have been proved as a key factor for designing and optimizing a better biofilm system. The most common carriers are plastics, gravels, and ceramsite, and they are relatively neutral (Cao et al., 2018; Morató et al., 2014; Torresi et al., 2016). Straw, polycaprolactone, corncobs, and hemp fiber are other carriers in the biofilm system (Andersson and Björnsson, 2002; Wang and Yang, 2013; Xu et al., 2009). These carriers are biodegradable and serve as slow-release carbon sources.

Recently, integrated-remediation technologies based on iron for cleaning up contaminated water have received much attention (Raji et al., 2021; Wu et al., 2019; Zhao et al., 2021). However, the iron serving as biofilm carriers for degrading toxic compounds was much less studied. Unlike the plastic carriers, iron carrier is more chemically active in natural surroundings due to the nature of easy corrosion (He et al., 2018; Kooij van der et al., 2020; LeChevallier et al., 1993). On the one hand, zero-valent iron and its ferric oxides may serve as electron donors and electron acceptors for microbial respiration (Ding et al., 2008; Liu et al., 2020). On the other hand, iron is essential for bacteria and can serve as a signal in biofilm development (Banin et al., 2005). In addition, the redox potential of Fe^{2+}/Fe^{3+} makes iron extremely versatile when it is incorporated into proteins as a catalytic center or as an electron carrier (Imbert and Blondeau, 1998; Pandey et al., 1994). Therefore, integrated remediation of zero valent iron and biofilm may have great potential in removing toxic compounds.

To test our hypothesis, two vertical baffled biofilm reactors (VBBR) with iron-carriers (Fe-VBBR) and plastic-carriers (Plastic-VBBR) were adopted for *p*-nitrophenol (PNP) degradation. PNP was selected as the target contaminant because of its environmental risks and wide distribution in industrial wastewater and groundwater (Subashchandrabose et al., 2018; Truong et al., 2021). In addition, the aromatic nitro group in PNP is an extremely good electron acceptor, and the nitro group can be reduced to an amino group by bacteria in the presence of sodium acetate. But, the phenol moiety is a good electron donor, which makes PNP particularly suited to study the above processes. The objectives of this study were the following: (1) to evaluate the effects of Fe-carriers and Plastic-carriers on biofilm formation; (2) to compare the kinetics of PNP degradation in two VBBR; (3) using next generation high-throughput sequencing to explore key genes involved in bacterial iron uptake.

2. Material and methods

2.1. Chemicals

PNP, KH_2PO_4, sodium acetate, and NH_4Cl were purchased from Shanghai Titan Scientific Co., Ltd. (Shanghai, China). All chemicals used were of the highest purity grade. Two reactors were fed with synthetic wastewater, containing 192.3 mg L^{-1} NH_4Cl, 11.3 mg L^{-1} KH_2PO_4, 126 mg L^{-1} $MgSO_4{\cdot}7H_2O$, 75.6 mg L^{-1} $CaCl_2{\cdot}2H_2O$ and trace element solution without $FeSO_4$ addition (0.25 μg L^{-1} $CuSO_4{\cdot}5H_2O$, 0.4 μg L^{-1} $ZnSO_4{\cdot}7H_2O$, 0.2 μg L^{-1} $CoCl{\cdot}6H_2O$, 1 μg L^{-1} $MnCl_2{\cdot}4H_2O$, 0.2 μg L^{-1} $NaMoO_4{\cdot}2H_2O$, 0.2 μg L^{-1} $NiCl_2{\cdot}6H_2O$, 0.2 μg L^{-1} $NaSeO_4{\cdot}10H_2O$, 25 μg L^{-1} EDTA and 0.01 μg L^{-1} H_3BO_4). PNP was added to the reactor tank by dilution from a stock solution (1000 mg L^{-1}). Sodium acetate was added directly by weighing sodium acetate powder.

2.2. VBBR configuration

A schematic diagram of the VBBR used in this study was presented in Fig. 1. The Fe-carriers are made of iron plates (mild steel), and the Plastic-carriers are made of plexiglass plates (polyvinyl chloride). These biofilm carriers had an identical size (diameter: 40 ± 2 mm, thickness: 3 ± 0.2 mm) with a D-shaped plate appearance. The D-shaped plates were fixed on a stainless steel rod by stainless steel nuts. The right VBBR had a working volume of 0.3 L, containing 15 iron carriers with a total exposed surface area of 0.03 m^2. The left VBBR had a volume of 0.3 L as well, containing 15 Plastic-carriers with a total exposed surface area of 0.03 m^2.

2.3. Experimental setup

A long-term acclimated activated sludge with sodium acetate and PNP addition over 10 months was sampled as inoculum to form biofilm. In brief, the supernatant of activated sludge was daily replaced by fresh medium containing sodium acetate (3 mM) and PNP (14 mg L^{-1}) during the process of activated sludge acclimation. The enriched PNP degrading inoculum was fed into two reactors for biofilm formation. The temperature was set at 30 °C in the air conditioner room and pH was kept at 7.0 ± 0.5 by phosphate buffer solution (PBS). The average dissolved oxygen concentration (DO) of 7.5 ± 0.5 mg L^{-1} could be maintained by a magnetic stirring. Two additional reactors without biofilm were performed as a control experiment to assess abiotic degradation of PNP.

2.4. Batch operation

A batch experiment was performed to assess the difference of PNP degradation in two VBBRs. To compare the kinetics of PNP degradation, PNP was degraded with four concentrations of sodium acetate (0, 1.2, 3, and 6 mM) addition. The biofilm grown on the Fe-carriers and Plastic-carriers was harvested for high-throughput sequencing analysis after the batch experiment was finished. The inoculum sample was collected before biofilm formation. The collected 3 samples were immediately cryopreserved at −20 °C prior to further DNA extraction and metagenome sequencing.

2.5. High-throughput sequencing

The genomic DNA was extracted using the Qiagen DNeasy PowerSoil Kit (QIAGEN GmbH, Hilden, Germany) according to the manufacturer's instructions. The purity and concentration of the extracted DNA samples were quantified using NanoDrop-2000 (Thermo Fisher Scientific, USA), and the quality was verified using gel electrophoresis with 0.8% agarose. The purified DNA samples were sent to Shanghai Personal Biotechnology Co., Ltd. (Shanghai, China) to perform high-throughput

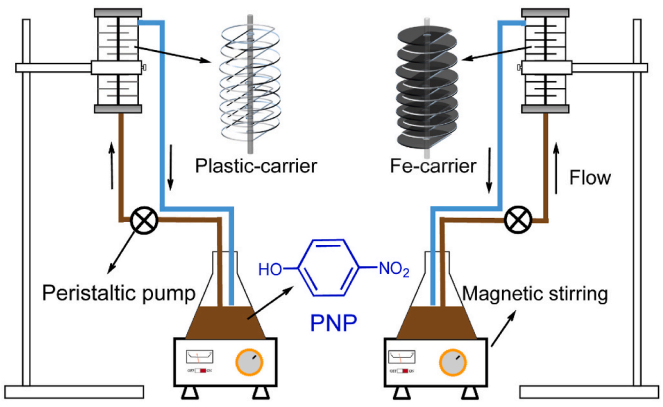

Fig. 1. Schematic diagram of the Plastic-VBBR (left) and the Fe-VBBR (right).

sequencing using Illumina MiSeq sequencing protocols. The data were processed by using QIIME (Quantitative Insights Into Microbial Ecology, version 1.8.0 http://qiime.org/) (Caporaso et al., 2010). The metagenomic functional composition prediction analysis for all samples from 16S data in the latest Kyoto Encyclopedia of Genes and Genomes (KEGG) database was performed using the PICRUSt2 pipeline as described by Langille et al. (2013).

2.6. Analytical methods

PNP was measured by a high performance liquid chromatography unit (HPLC, UltiMate 3000, Thermo Scientific, DIONEX, USA) equipped with a UV detector and an auto-sampler and with an Agilent TC-C18 column (4.6*250 mm) at 30 °C. The mobile phase was methanol: water (60:40, V/V) with a flow rate of 1.0 mL min^{-1}, and the UV wavelength for detection was 254 nm. The detection limit of PNP was 0.14 μM L^{-1}. Water samples (1 mL) were collected by disposable syringe and filtered immediately through 0.22 μm membrane filters (LC + PES membrane, Pall Life Sciences Acrodisc Syringe Filters, USA). No PNP adsorption on the membrane filter was observed by HPLC. pH and DO were measured by a portable pH/DO/temperature meter (HACH, HQ 30d, USA) with a gel-filled pH electrode and DO electrode.

The rates of PNP removal (k_{PNP}) with four acetate concentrations addition in two VBBRs were calculated by a linear fit. The fitting equation is y = a + k*x. The k presents k_{PNP} with a unit: μM L^{-1} h^{-1}.

2.7. CLSM imaging of biofilm

Biofilms grown on the two kinds of carriers in the VBBR were measured using a confocal laser scanning microscopy (CLSM) instrument (Zeiss LSM980 Airyscan2). The fluorescence of the biofilm was observed with excitation at 488 nm and emission at 509 nm. Biofilm staining was conducted according to the protocol provided by Calcein-AM/PI Bacterial Viability Kit (Solarbio, CA1630, Beijing, China). The CLSM images were analyzed using IMARIS (version 9.3.1, Bitplane, Zurich, Switzerland) to calculate biofilm thickness.

2.8. Accession numbers

The 16SrRNA gene sequences of three sample have been deposited in NCBI Genbank under the project: PRJNA788203.

3. Results and discussion

3.1. Biofilm formation and characteristic of bacterial community

Compared to the Plastic-carriers, a thick biofilm was formed on the surface of iron plates in the Fe-VBBR after four weeks (Fig. 2B). The average thickness of biofilm on the Plastic-carrier was 99.5 μm, and the maximum thickness was 164 μm. However, the average thickness of biofilm was 145 μm for the Fe-carriers (maximum thickness, 412 μm). This result suggests that Fe-carriers enhanced biofilm development. Iron is essential for bacteria and serves as a signal for biofilm development (Singh, 2004; Singh et al., 2002). Research reported that the maximum Fe concentration on mild steel was 750 μg Fe cm^{-2} within 15 days when exposure to tap water (Kooij van der et al., 2020). In this study, the rate of biofilm formation on the Fe-carriers was faster than that on the Plastic-carriers. The Fe-carriers could release Fe^{2+}/Fe^{3+} into the solution to provide iron for enhancing biofilm formation. This result was similar to the latest research that mild steel pipes exposed to intermittently flowing tap water can promote biofilm formation (Kooij van der et al., 2020).

Compared to the inoculum, the biodiversity of the bacterial community in the two VBBRs decreased, but the biodiversity of the bacterial community in the Fe-VBBR was higher than that in the Plastic-VBBR (Fig. 3). It suggests that many species were phased out during PNP-degrading bacteria acclimation. Community biodiversity is a complex concept, including richness and evenness (Wittebolle et al., 2009). The richness of the bacterial community between two VBBRs was very similar (Fig. 3C and D), while the evenness of the bacterial community in the Fe-VBBR was higher than that in the Plastic-VBBR (Fig. 3A and B). The Chao1 index in the Fe-VBBR was 2.4% higher than that in the Plastic-VBBR. The ACE index was 933 in the Fe-VBBR and was 928 in the Plastic-VBBR. The Shannon index in the Fe-VBBR was 13.4% higher than that in the Plastic-VBBR. A lower Simpson index represents a higher evenness of the bacterial community. The Simpson index in the Fe-VBBR was 43.8% lower than that in the Plastic-VBBR. The evenness of microbial community is a key factor in preserving the functional stability of an ecosystem. The microbial communities with higher evenness was found to have higher functionality and stability than microbial communities with lower evenness (Wittebolle et al., 2009). This indicates that biofilm grown on the Fe-carriers had a higher functionality and stability than that on the Plastic-carriers.

The biofilm thickness and biodiversity are positively associated with the removal of some pollutants (Johnson David et al., 2015; Torresi et al., 2016). Biofilm formation is affected by a variety of factors, including the nature of carrier materials. Bacterial growth on surfaces of mild steel pipes exposed to drinking water is a well-known phenomenon in practice (Rogers et al., 1994). This phenomenon is undesirable because the growth of the organism in potable water supplies may lead to human infection (Cassini et al., 2018). But information about the rate of biofilm formation on the different pumping materials provide many directions to enhance biofilm formation. Batch tests confirmed that a variety of pumping materials, including plasticized PVC, polyethylene, polypropylene and mild steel in contact with tap water enhanced bacterial growth as compared to glass, stainless steel and copper (Kooij van der et al., 2020; Rogers et al., 1994). However, the release of corrosion by-products with attached biomass from mild steel most likely enhanced biofilm formation as compared to plastic and copper materials (Kooij van der et al., 2020). Therefore, iron is very suitable as a biofilm carrier to enhance the removal of pollution in biofilm-based system.

3.2. PNP degradation by Achromobacter dominated community

Faster rates of PNP degradation were observed in the Fe-VBBR with four concentrations of acetate addition (Fig. 4). As the acetate concentrations increased from 0 mM to 6 mM, k_{PNP} values rapidly increased in the Fe-VBBR. The Fe-VBBR reached a maximal k_{PNP} value at 13.02 μM

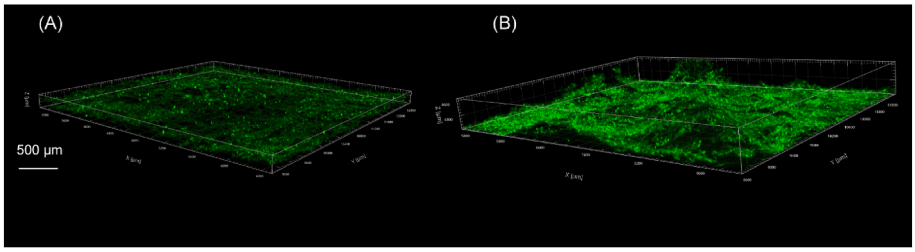

Fig. 2. CLSM images of biofilms formed on the Plastic-carriers (A) and the Fe-carriers (B) after four weeks. The scale bar represents 500 μm.

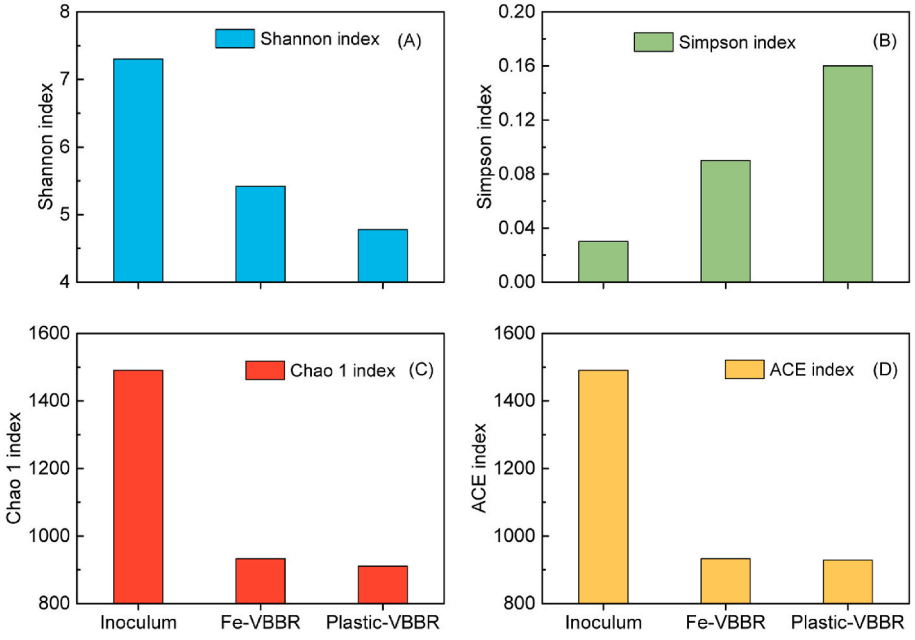

Fig. 3. The indexes of biodiversity in the Inoculum and two VBBRs. (A) Shannon's diversity index; (B) Simpson's diversity index; (C) Chao 1's richness index; (D) ACE's richness index.

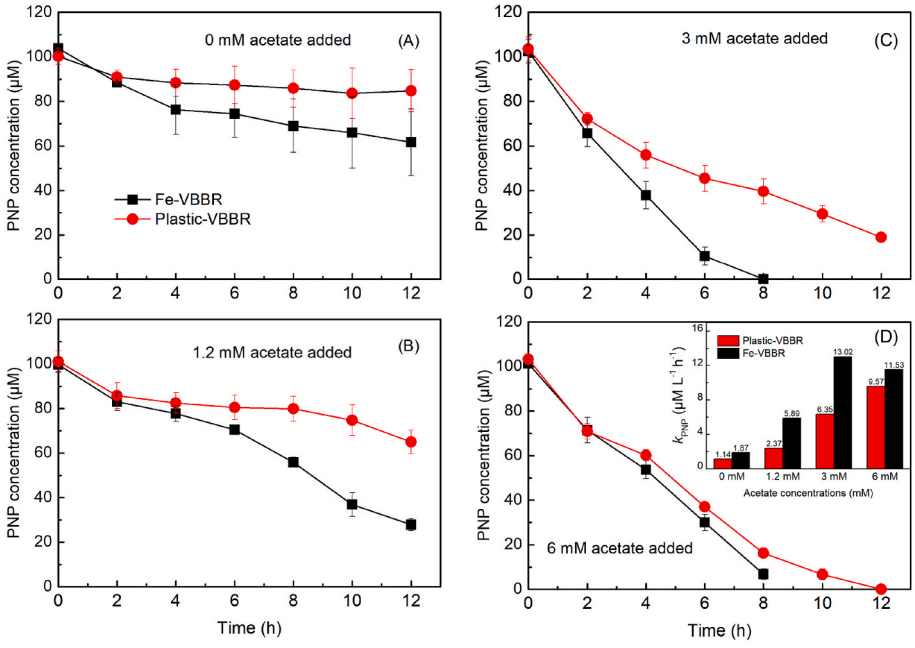

Fig. 4. Variation of PNP Concentrations with the time in two VBBRs. All tests with initial PNP concentrations of 100 ± 5 μM. Sodium acetate concentration were as follows: (A) 0 mM sodium acetate added; (B) 1.2 mM sodium acetate added; (C) 3 mM sodium acetate added; (D) 6 mM sodium acetate added. All experiments were repeated three times in batch mode for avoiding uncertainty. The inset showed k_{PNP} values when four acetate concentrations were supplemented into two VBBRs.

L^{-1} h^{-1} with 3 mM sodium acetate addition (Fig. 4C), which was 1.05 fold higher than that in the Plastic-VBBR. The maximal k_{PNP} value in the Plastic-VBBR was only 9.57 μM L^{-1} h^{-1} when 3 mM sodium acetate was added (Fig. 4 D). This suggests that PNP degradation was enhanced by Fe-carriers in the Fe-VBBR.

The bacterial community was analyzed for interpreting the pathway of PNP degradation. Proteobacteria was highly enriched and became the dominant phylum in two VBBRs (Fig. 5A). The relative abundance was 91.7% in the Plastic VBBR and was 77.1% in the Fe-VBBR. Proteobacteria plays an important role in contaminants removal (Zhou et al., 2015). Proteobacteria in two VBBRs increased by 93.9% in the Plastic-VBBR and by 63.0% in the Fe-VBBR, while Actinobacter in two VBBRs decreased by 69.5% in the Plastic-VBBR and by 46.3% in the Fe-VBBR. Similarly, Planctomycetes decreased by 92.0% in the Plastic-VBBR and decreased by 33.0% in the Fe-VBBR.

The functional bacteria at the genus/family level were investigated to identify PNP degraders in two VBBRs. *Achromobacter*, which is known as PNP degrader (Wan et al., 2007), took up the largest proportion in two VBBRs (Plastic-VBBR, 46.5%; Fe-VBBR, 24.9%), although the initial relative abundance was only 0.3% in the Inoculum (Fig. 5B).

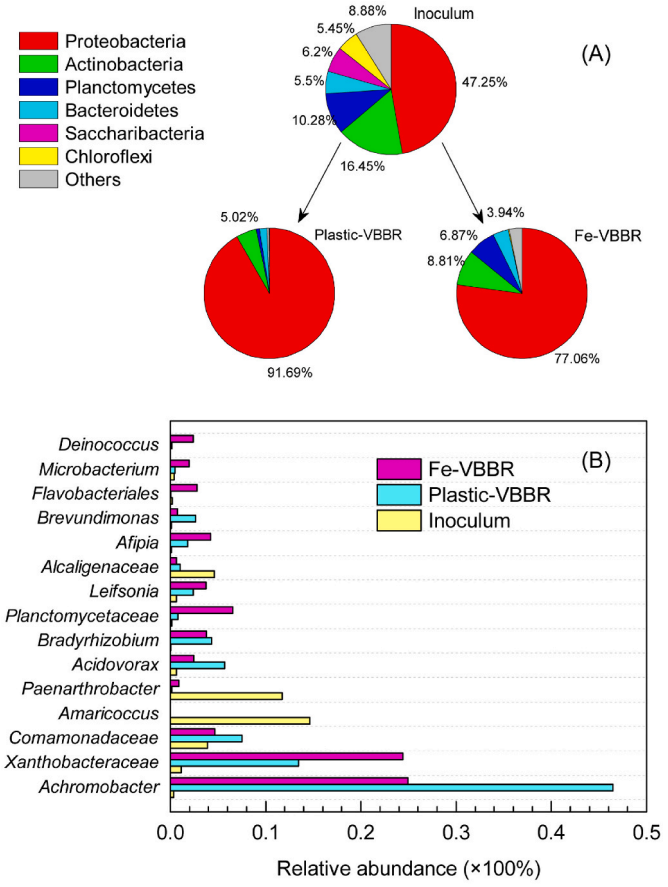

Fig. 5. Proportion of the top 5 phyla in the bacterial communities was reshaped by two kinds of carriers. The relative abundances of the top 15 genera were compared among three bacterial communities.

Achromobacter xylosoxidans Ns strain is capable of utilizing PNP as the sole source of carbon, energy, and nitrogen (Wan et al., 2007). The pathway of PNP degradation in *Achromobacter* involves 4-nitrocatechol, 1,2,4-benzenetriol, and maleylacetate as major degradation intermediates (Chauhan et al., 2010; Wan et al., 2007). *Achromobacter* became the dominant species in biofilm, which demonstrates that *Achromobacter* was the main PNP degrader.

A potential PNP degrader was the Xanthobacteraceae family, because this family was highly enriched. The norank genus from the Xanthobacteraceae family accounted for 24.4% of the bacterial community in the Fe-VBBR and accounted for 13.5% in the Plastic-VBBR (Inoculum, 1.1%). Although PNP degraders within the Xanthobacteraceae family were not reported by previous literature, members within the Xanthobacteraceae family are capable of degrading aromatic compounds and have a gene with homology to catechol 2,3-dioxygenase (Marín et al., 2019). Thinks to PNP as a typical aromatic compound, the Xanthobacteraceae family might play an important role in degrading PNP and its intermediates in two VBBRs.

The Comamonadaceae family was also enriched in two VBBRs (7.5% in the Plastic-VBBR and 4.7% in the Fe-VBBR). A strain within the Comamonadaceae family is able to metabolize 1-chloro-4-nitrobenzene (Boon et al., 2001). PNP and 1-chloro-4-nitrobenzene share the same moiety of nitrobenzene, so *Comamonadaceae* might account for degrading PNP and its products in this study.

Other increased genera involved in PNP degradation in two VBBRs included *Acidovorax*, *Bradyrhizobium*, and *Leifsonia*. *Acidovorax* shows broad degradation ability toward mono-nitrophenols (Kawagoshi et al., 2006; Zhao and Ward, 1999). *Bradyrhizobium*, which was only observed in two VBBRs, is capable of biodegrading synthetic dyes and other nitro-aromatic compounds (Qu and Spain, 2010). *Leifsonia* is responsible for encoding alcohol dehydrogenase, which plays an important role in aromatic compound conversion (Inoue et al., 2006). These increased genera might cooperatively degrade PNP and products via the same and different catabolism pathways in two VBBRs.

Deinococcus radiodurans is the most radiation-resistant organism discovered to date (Fredrickson et al., 2000). The genus *Deinococcus* can reduce Fe(III) coupled to the oxidation of organic compounds (Fredrickson et al., 2000). This genus only occurred in two VBBRs with a relative abundance of 2.4% in the Fe-VBBR and 0.1% in the Plastic-VBBR, respectively. In this study, the occurrence of *Deinococcus* implied that Fe-carriers released Fe(III) into the solution by corroding. Small *Deinococcus* in the Plastic-VBBR ascribed a little of Fe(III) released from an iron rod which was used for fixing carriers (Fig. 2).

Alpha diversity analysis revealed that biofilm grown on the Fe-carriers was more rich and even than that on the Plastic-carriers. Both richness and evenness are positively associated with the removal of pollutants in full-scale wastewater treatment (Johnson David et al., 2015). In a heterogeneous (higher biodiversity) biofilm system, biodegradation capability may be more robust than the single-cell dominant ones as not only could different microorganisms have the same catabolic pathways but also within the consortia there might be different pathways that can degrade PNP (Garcia-Becerra and Ortiz, 2018; Hu et al., 2017). Therefore, *Achromobacter* dominated biofilm grown on the Plastic-carriers with lower evenness had a slower rate of PNP removal.

3.3. KEGG orthology reveals iron roles in PNP degradation

Iron is important for numerous biological processes which include respiration, oxygen transport, DNA biosynthesis, gene regulation, etc. (Krewulak and Vogel, 2008). Abundances of four key genes for encoding iron transport protein except for substrate-binding protein genes were increased under an iron-limited condition in two VBBRs (Fig. 6). This suggests that bacteria positively upregulated the gene expression of ferric uptake regulator to the fulfill nutritional requirement for iron. Compared to the Fe-VBBR, the iron-limited condition was more severe in the Plastic-VBBR. Under iron-limited conditions, bacteria synthesize low molecular weight iron-chelating compounds known as siderophores which scavenge iron from precipitates in the microorganism's extracellular milieu. However, these ferric-siderophore complexes exceed the molecular weight cut off of porins and require specific outer membrane receptors for iron uptake into the periplasmic space. Therefore, the abundance of genes for encoding outer membrane receptor protein in the Plastic-VBBR was 31.7% higher than that in the Fe-VBBR, which assisted more siderophores into the periplasm (Fig. 6A). Additionally, the abundances of genes for encoding the periplasmic binding protein, permease protein, and ATP-binding protein in the Fe-VBBR were higher than those in the Plastic-VBBR, and thus more iron was transported into the cytoplasm. These results reveal that iron played an important role in regulating biofilm formation and degrading PNP.

3.4. Abundances of key genes in the pathway of PNP degradation

Achromobacter xylosoxidans Ns is as a PNP degrader through an initial hydroxylation on carbon 2 followed by the release of the nitro group (Wan et al., 2007). 4-nitrocatechol and 1,2,4-benzenetriol are as identified products. Similar pathway of PNP degradation via 4-nitrocatechol and 1,2,4-benzenetriol by a Gram-negative bacterium, *Burkholderia* sp. SJ98 was reported (Chauhan et al., 2010). Although two characterized genes (K21726 and K21727) were identified as a PNP 2-monooxygenase in a Gram-positive bacterium, *Rhodococcus opacus* SAO101 (Kitagawa et al., 2004), they didn't occur in three samples. This implies that a new gene for transforming PNP to 4-nitrocatechol in a Gram-negative bacterium, *Achromobacter* was different from *Rhodococcus*. Other genes for catalyzing 1,2,4-benzenetriol metabolism to the

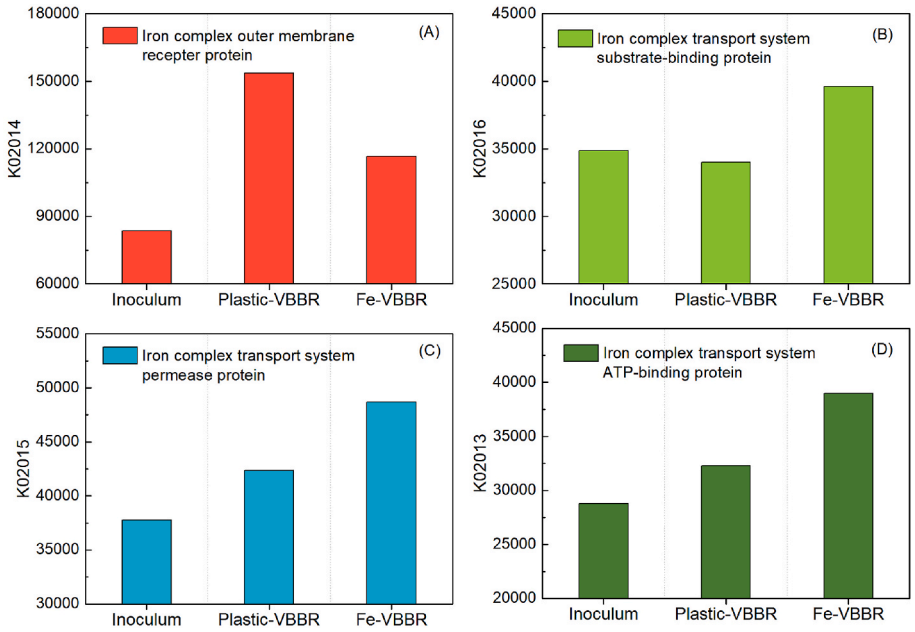

Fig. 6. Abundances of four key genes involved in ferric uptake suggested these genes for encoding iron uptake transporter proteins increased under iron-limited conditions. The iron sources are transported into Gram-negative bacterial cells via specific uptake pathways which include an outer membrane receptor protein (K02014), a substrate-binding protein (K02016), a permease protein (K02015), and an inner membrane ATP-binding protein (K02013).

citrate cycle were observed (Fig. 7).

Abundances of genes involved in transforming PNP intermediates increased in two VBBRs, while their abundances except for 3-oxoadipate CoA-transferase genes (K01031 and K01032) in the Fe-VBBR were higher than those in the Plastic-VBBR (Fig. 8). The genes for encoding hydroxyquinol 1,2-dioxygenase (K04098) increased by 6-fold in the Plastic-VBBR and by 13-fold in the Fe-VBBR (Fig. 8A). Maleylacetate reductase genes also increased by 1.5-fold in the Plastic-VBBR and by 2.1-fold in the Fe-VBBR. Two pathways cooperatively transferred 3-oxoadipate-CoA via Acetyl-CoA acyltransferase (K00632) and 3-oxoadipyl-CoA thiolase (K07823) into the citrate cycle (Fig. 7). The Acetyl-CoA pathway was dominant because the much higher abundance of Acetyl-CoA acyltransferase genes was observed (Fig. 8E and F). These results suggest that the PNP degradation was enhanced by biofilm bioreactor, but the Fe-VBBR expressed more genes to accelerate PNP transformation.

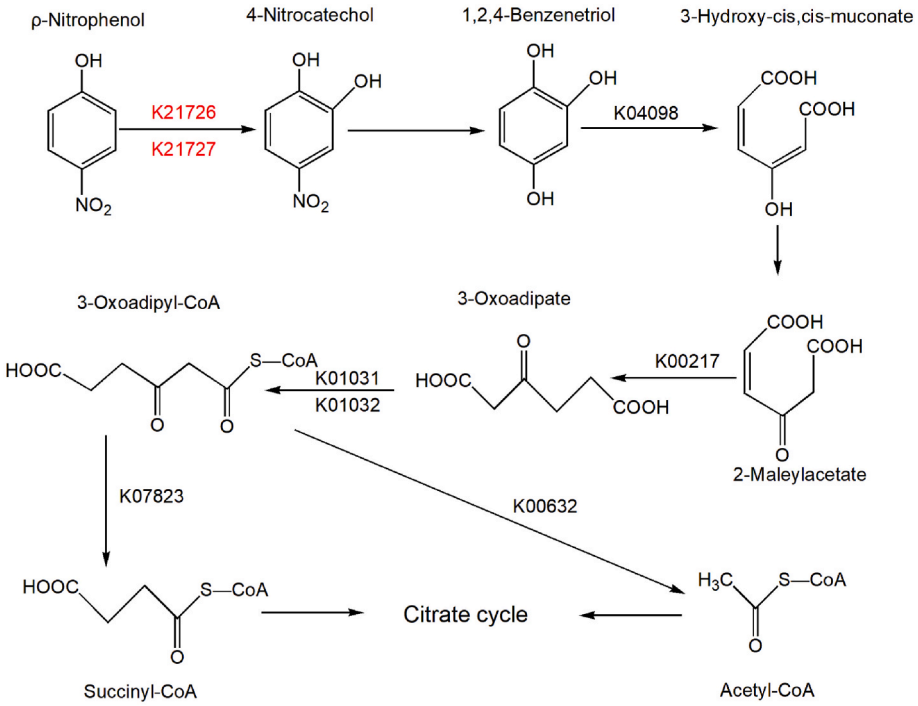

Fig. 7. Proposed metabolic pathway for PNP degradation according to KEGG pathway of PNP degradation. Each step of PNP degradation was catalyzed by specific genes/proteins (K number). Note, K numbers written with red font present absence in the pathway of PNP degradation in this study. (For interpretation of the references to colour in this figure legend, the reader is referred to the Web version of this article.)

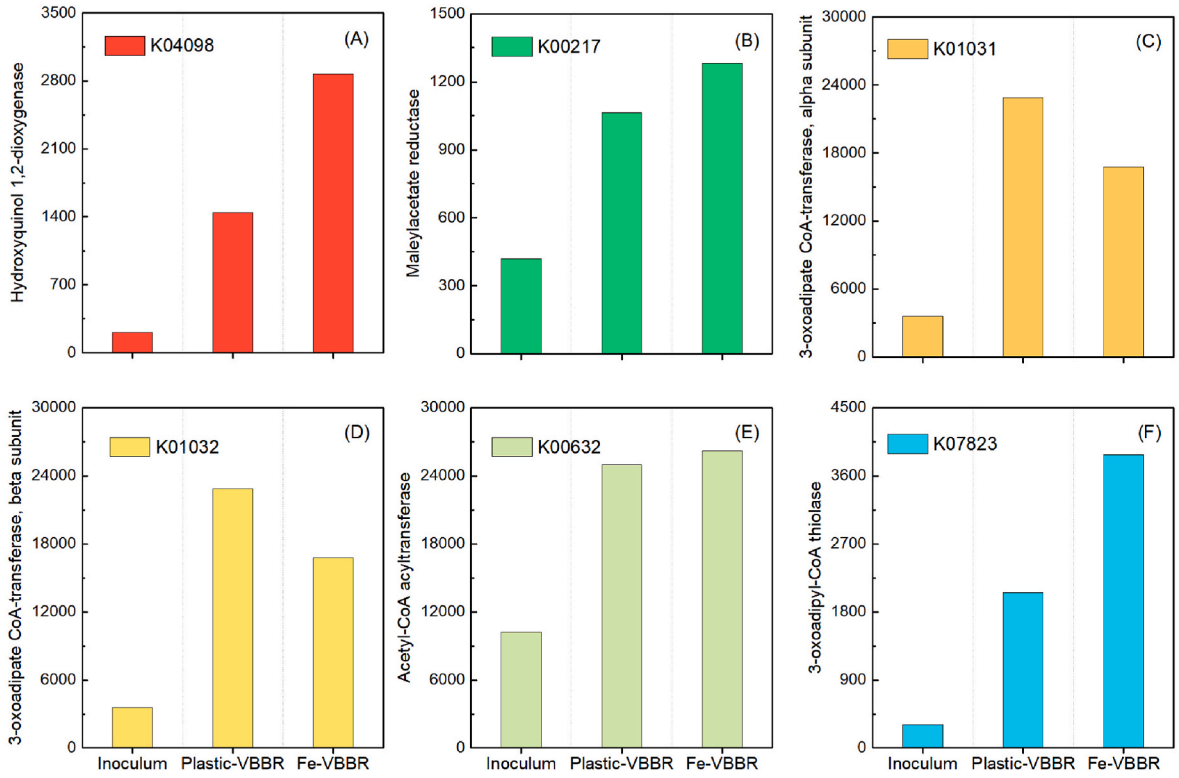

Fig. 8. Abundances of genes for PNP degradation in three samples.

4. Conclusions

This study confirmed that iron carriers played an important role in enhancing biofilm formation and PNP degradation. The maximum thickness of biofilm grown on the Fe-carriers was 412 μm, while the maximum thickness of biofilm was 164 μm for the Plastic-carriers. Additionally, the Fe-carriers increased the evenness of the bacterial community. The maximum rate of PNP removal reached at 13.02 μM L^{-1} h^{-1} with 3 mM sodium acetate addition in the Fe-VBBR, versus 11.53 μM L^{-1} h^{-1} with a higher concentration of 6 mM sodium acetate addition in the Plastic-VBBR. *Achromobacter* genus and Xanthobacteraceae family may be as main PNP degraders in two VBBRs. More iron uptake genes involved in iron uptake were expressed for fulfilling the nutritional requirement for iron under an iron-limited condition in two VBBRs. PNP transformed via 4-nitrocatechol and 1,2,4-benzenetriol and entered into the citrate cycle mainly via acetyl-CoA.

Credit author statement

Lifeng Cao: Investigation, Resources, Software, Writing – original draft, Formal analysis, Visualization. Ge Zhu: Investigation, Resources. Jinzhao Tao: Resources. Yongming Zhang: Conceptualization, Supervision, Writing – review & editing, Methodology.

Declaration of competing interest

The authors declare that they have no known competing financial interests or personal relationships that could have appeared to influence the work reported in this paper.

Acknowledgements

The authors acknowledge the financial support of the ability construction project of local Colleges and Universities in Shanghai (16070503000), Special Fund of State Key Joint Laboratory of Environment Simulation and Pollution Control (16K10ESPCT) and Shanghai Gaofeng & Gaoyuan Project for University Academic Program Development.

References

Andersson, J., Björnsson, L., 2002. Evaluation of straw as a biofilm carrier in the methanogenic stage of two-stage anaerobic digestion of crop residues. Bioresour. Technol. 85 (1), 51–56.
Banin, E., Vasil, M.L., Greenberg, E.P., 2005. Iron and Pseudomonas aeruginosa biofilm formation. Proc. Natl. Acad. Sci. Unit. States Am. 102 (31), 11076–11081.
Boon, N., Goris, J., De Vos, P., Verstraete, W., Top, E.M., 2001. Genetic diversity among 3-chloroaniline- and aniline-degrading strains of the Comamonadaceae. Appl. Environ. Microbiol. 67 (3), 1107–1115.
Cao, L., Zhang, C., Zou, S., Zhu, G., Li, N., Zhang, Y., Rittmann, B.E., 2018. Simultaneous anaerobic and aerobic transformations of nitrobenzene. J. Environ. Manag. 226, 264–269.
Caporaso, J.G., Kuczynski, J., Stombaugh, J., Bittinger, K., Bushman, F.D., Costello, E.K., Fierer, N., Peña, A.G., Goodrich, J.K., Gordon, J.I., Huttley, G.A., Kelley, S.T., Knights, D., Koenig, J.E., Ley, R.E., Lozupone, C.A., McDonald, D., Muegge, B.D., Pirrung, M., Reeder, J., Sevinsky, J.R., Turnbaugh, P.J., Walters, W.A., Widmann, J., Yatsunenko, T., Zaneveld, J., Knight, R., 2010. QIIME allows analysis of high-throughput community sequencing data. Nat. Methods 7 (5), 335–336.
Cassini, A., Högberg, L.D., Plachouras, D., Quattrocchi, A., Hoxha, A., Simonsen, G.S., 2018. Attributable deaths and disability-adjusted life-years caused by infections with antibiotic-resistant bacteria in the EU and the European Economic Area in 2015: a population-level modelling analysis. Lancet Infect. Dis. 18, 1–11.
Chauhan, A., Pandey, G., Sharma, N.K., Paul, D., Pandey, J., Jain, R.K., 2010. p-Nitrophenol degradation via 4-nitrocatechol in Burkholderia sp. SJ98 and cloning of some of the lower pathway genes. Environ. Sci. Technol. 44 (9), 3435–3441.
de Beer, D., Stoodley, P., Roe, F., Lewandowski, Z., 1994. Effects of biofilm structures on oxygen distribution and mass transport. Biotechnol. Bioeng. 43 (11), 1131–1138.
Ding, Y.H.R., Hixson, K.K., Aklujkar, M.A., Lipton, M.S., Smith, R.D., Lovley, D.R., Mester, T., 2008. Proteome of Geobacter sulfurreducens grown with Fe(III) oxide or Fe(III) citrate as the electron acceptor. Biochim. Biophys. Acta Protein Proteonomics 1784 (12), 1935–1941.
Dutta, L., Nuttall, H., Cunningham, A., James, G., Hiebert, R., 2005. In situ biofilm barriers: case study of a nitrate groundwater plume, Albuquerque, New Mexico. Remed. J. 15, 101–111.
Flemming, H.C., Wingender, J., 2010. The biofilm matrix. Nat. Rev. Microbiol. 8 (9), 623–633.
Fredrickson, J.K., Kostandarithes, H.M., Li, S.W., Plymale, A.E., Daly, M.J., 2000. Reduction of Fe(III), Cr(VI), U(VI), and Tc(VII) by Deinococcus radiodurans R1. Appl. Environ. Microbiol. 66 (5), 2006–2011.

Garcia-Becerra, F.Y., Ortiz, I., 2018. Biodegradation of emerging organic micropollutants in nonconventional biological wastewater treatment: a critical review. Environ. Eng. Sci. 35 (10), 1012–1036.
He, C., He, D., Collins, R.N., Garg, S., Mu, Y., Waite, T.D., 2018. Effects of good's buffers and pH on the structural transformation of zero valent iron and the oxidative degradation of contaminants. Environ. Sci. Technol. 52 (3), 1393–1403.
Hu, P., Dubinsky, E.A., Probst, A.J., Wang, J., Sieber, C.M.K., Tom, L.M., Gardinali, P.R., Banfield, J.F., Atlas, R.M., Andersen, G.L., 2017. Simulation of Deepwater Horizon oil plume reveals substrate specialization within a complex community of hydrocarbon degraders. Proc. Natl. Acad. Sci. Unit. States Am. 114 (28), 7432–7437.
Imbert, M., Blondeau, R., 1998. On the iron requirement of lactobacilli grown in chemically defined medium. Curr. Microbiol. 37 (1), 64–66.
Inoue, Kousuke, Makino, Yoshihide, Dairi, Tohru, Itoh, Nobuya, 2006. Gene Cloning and Expression of Leifsonia Alcohol Dehydrogenase (LSADH) Involved in Asymmetric Hydrogen-Transfer Bioreduction to Produce (R)-Form Chiral Alcohols. Biosci. Biotechnol. Biochem. 70 (2), 418–426.
Jamal Khan, S., Zohaib Ur, R., Visvanathan, C., Jegatheesan, V., 2012. Influence of biofilm carriers on membrane fouling propensity in moving biofilm membrane bioreactor. Bioresour. Technol. 113, 161–164.
Johnson David, R., Helbling Damian, E., Lee Tae, K., Park, J., Fenner, K., Kohler Hans-Peter, E., Ackermann, M., Spormann, A.M., 2015. Association of biodiversity with the rates of micropollutant biotransformations among full-scale wastewater treatment plant communities. Appl. Environ. Microbiol. 81 (2), 666–675.
Kawagoshi, Y., Fukuda, J., Takahashi, H., Fujimoto, A., Minami, N., Furukawa, K., 2006. Treatment of p-nitrophenol-containing wastewater using fluidized bed reactor with polyvinyl alcohol (PVA) gel beads. J. Jpn. Soc. Water Environ. 29 (9), 547–552.
Kim, M.H., 2016. Nanoparticle-based therapies for wound biofilm infection: opportunities and challenges. IEEE Trans. NanoBioscience 15, 1-1.
Kitagawa, W., Kimura, N., Kamagata, Y., 2004. A novel p-nitrophenol degradation gene cluster from a gram-positive bacterium, Rhodococcus opacus SAO101. J. Bacteriol. 186 (15), 4894–4902.
Kooij van der, D., Veenendaal, H.R., Italiaander, R., 2020. Corroding copper and steel exposed to intermittently flowing tap water promote biofilm formation and growth of Legionella pneumophila. Water Res. 183, 115951.
Krewulak, K.D., Vogel, H.J., 2008. Structural biology of bacterial iron uptake. Biochim. Biophys. Acta Biomembr. 1778 (9), 1781–1804.
Kwok, W., Picioreanu, C., Ong, S.L., Van Loosdrecht, M., Ng, J., Heijnen, S., 1998. Influence of biomass production and detachment forces on biofilm structures in a biofilm airlift suspension reactor. Biotechnol. Bioeng. 58, 400–407.
Langille, M.G.I., Zaneveld, J., Caporaso, J.G., McDonald, D., Knights, D., Reyes, J.A., Clemente, J.C., Burkepile, D.E., Vega Thurber, R.L., Knight, R., Beiko, R.G., Huttenhower, C., 2013. Predictive functional profiling of microbial communities using 16S rRNA marker gene sequences. Nat. Biotechnol. 31 (9), 814–821.
LeChevallier, M.W., Lowry, C.D., Lee, R.G., Gibbon, D.L., 1993. Examining the relationship between iron corrosion and the disinfection of biofilm bacteria. J. AWWA (Am. Water Works Assoc.) 85 (7), 111–123.
Liang, Y., Jiao, C., Pan, L., Zhao, T., Liang, J., Xiong, J., Wang, S., Zhu, H., Chen, G., Lu, L., Song, H., Yang, Q., Zhou, Q., 2021. Degradation of chlorine dioxide bleaching wastewater and response of bacterial community in the intimately coupled system of visible-light photocatalysis and biodegradation. Environ. Res. 195, 110840.
Liu, C., Faria, A.F., Ma, J., Elimelech, M., 2017. Mitigation of biofilm development on thin-film composite membranes functionalized with zwitterionic polymers and silver nanoparticles. Environ. Sci. Technol. 51 (1), 182–191.
Liu, C.S., Li, W., Liu, L.H., Yu, H.T., Liu, F., Lee, D.J., 2020. Autotrophic induced heterotrophic bioreduction of bromate in use of elemental sulfur or zerovalent iron as electron donor. Bioresour. Technol. 317, 124015.
Long, M., Ilhan, Z.E., Xia, S., Zhou, C., Rittmann, B.E., 2018. Complete dechlorination and mineralization of pentachlorophenol (PCP) in a hydrogen-based membrane biofilm reactor (MBfR). Water Res. 144, 134–144.
Marín, P., Martirani-Von Abercron, S.M., Urbina, L., Pacheco-Sánchez, D., Castañeda-Cataña, M.A., Retegi, A., Eceiza, A., Marqués, S., 2019. Bacterial nanocellulose production from naphthalene. Microb. Biotechnol. 12 (4), 662–676.
Mitchell, K.F., Zarnowski, R., Sanchez, H., Edward, J.A., Reinicke, E.L., Nett, J.E., Mitchell, A.P., Andes, D.R., 2015. Community participation in biofilm matrix assembly and function. Proc. Natl. Acad. Sci. Unit. States Am. 112 (13), 4092–4097.
Morató, J., Codony, F., Sánchez, O., Pérez, L.M., García, J., Mas, J., 2014. Key design factors affecting microbial community composition and pathogenic organism removal in horizontal subsurface flow constructed wetlands. Sci. Total Environ. 481, 81–89.
Pandey, A., Bringel, F., Meyer, J.M., 1994. Iron requirement and search for siderophores in lactic acid bacteria. Appl. Microbiol. Biotechnol. 40 (5), 735–739.
Qu, Y., Spain, J.C., 2010. Biodegradation of 5-nitroanthranilic acid by Bradyrhizobium sp. strain JS329. Appl. Environ. Microbiol. 76 (5), 1417–1422.
Raji, M., Mirbagheri, S.A., Ye, F., Dutta, J., 2021. Nano zero-valent iron on activated carbon cloth support as Fenton-like catalyst for efficient color and COD removal from melanoidin wastewater. Chemosphere 263, 127945.
Rittmann, B.E., 2018. Biofilms, active substrata, and me. Water Res. 132, 135–145.
Rogers, J., Dowsett, A.B., Dennis, P.J., Lee, J.V., Keevil, C.W., 1994. Influence of plumbing materials on biofilm formation and growth of Legionella pneumophila in potable water systems. Appl. Environ. Microbiol. 60 (6), 1842–1851.
Singh, P.K., 2004. Iron sequestration by human lactoferrin stimulates P. aeruginosa surface motility and blocks biofilm formation. Biometals 17 (3), 267–270.
Singh, P.K., Parsek, M.R., Greenberg, E.P., Welsh, M.J., 2002. A component of innate immunity prevents bacterial biofilm development. Nature 417 (6888), 552–555.
Subashchandrabose, S.R., Venkateswarlu, K., Krishnan, K., Naidu, R., Lockington, R., Megharaj, M., 2018. Rhodococcus wratislaviensis strain 9: an efficient p-nitrophenol degrader with a great potential for bioremediation. J. Hazard Mater. 347, 176–183.
Tan, C., Zeng, Q., Zhu, G., Ning, Y., Zhu, X., Zhang, P., Yan, N., Zhang, Y., Rittmann, B.E., 2021. Characteristics of denitrification in a vertical baffled bioreactor. Environ. Res. 197, 111046.
Torresi, E., Fowler, S.J., Polesel, F., Bester, K., Andersen, H.R., Smets, B.F., Plósz, B.G., Christensson, M., 2016. Biofilm thickness influences biodiversity in nitrifying MBBRs—implications on micropollutant removal. Environ. Sci. Technol. 50 (17), 9279–9288.
Truong, T.K., Nguyen, T.Q., Phuong La, H.P., Le, H.V., Van Man, T., Cao, T.M., Van Pham, V., 2021. Insight into the degradation of p-nitrophenol by visible-light-induced activation of peroxymonosulfate over Ag/ZnO heterojunction. Chemosphere 268, 129291.
Tsushima, I., Ogasawara, Y., Kindaichi, T., Satoh, H., Okabe, S., 2007. Development of high-rate anaerobic ammonium-oxidizing (anammox) biofilm reactors. Water Res. 41 (8), 1623–1634.
Wan, N., Gu, J., Yan, Y., 2007. Degradation of p-nitrophenol by Achromobacter xylosoxidans Ns isolated from wetland sediment. Int. Biodeterior. Biodegrad. 59 (2), 90–96.
Wang, H.M., Yang, F., 2013. Biological denitrification using slow-release carbon source composite materials as solid carbon source and biofilm carrier. Adv. Mater. Res. 702, 218–223.
Wang, W., Huang, Y., Liu, J., Peng, A., 2002. Effect of Some Environmental Factors on Mercury(II) Reduction by Suspended Particulate Matter-Associated Kluvera cryocrescens Biofilms in Waterbodies. Water Environ. Res. 74 (1), 77–81.
Wittebolle, L., Marzorati, M., Clement, L., Balloi, A., Daffonchio, D., Heylen, K., De Vos, P., Verstraete, W., Boon, N., 2009. Initial community evenness favours functionality under selective stress. Nature 458 (7238), 623–626.
Wu, J., Wang, B., Blaney, L., Peng, G., Chen, P., Cui, Y., Deng, S., Wang, Y., Huang, J., Yu, G., 2019. Degradation of sulfamethazine by persulfate activated with organo-montmorillonite supported nano-zero valent iron. Chem. Eng. J. 361, 99–108.
Xu, Z., Liu, S., Yin, H., Chu, H., Yao, Y., 2009. Biological denitrification using corncobs as a carbon source and biofilm carrier. Water Environ. Res. 81 (3), 242–247.
Zhao, J.S., Ward, O.P., 1999. Microbial degradation of nitrobenzene and mono-nitrophenol by bacteria enriched from municipal activated sludge. Can. J. Microbiol. 45 (5), 427–432.
Zhao, Q., Li, X., Xiao, S., Peng, W., Fan, W., 2021. Integrated remediation of sulfate reducing bacteria and nano zero valent iron on cadmium contaminated sediments. J. Hazard Mater. 406, 124680.
Zhou, A., Liu, W., Varrone, C., Wang, Y., Wang, A., Yue, X., 2015. Evaluation of surfactants on waste activated sludge fermentation by pyrosequencing analysis. Bioresour. Technol. 192, 835–840.